

## Chapter 3

### Genotoxic evaluation of Agrochemical on ICG cell line

#### 3.1 Introduction:

Biochemical markers of contamination are important indices used in fish toxicity tests and for field monitoring of aquatic pollution. They confirm contact of the specimen with specific groups of chemical compounds and clarify their further metabolic fate. Liver plays a key role in xenobiotic detoxication in fish. Polarity of a xenobiotic increases within two phases of metabolization through oxidation, reduction and hydrolysis reactions, subsequently the produced metabolite (or less frequently the originated compound) is conjugated with an endogenous substrate and excreted. The tissue specific presence of different types of p450 genes were reported in gills, kidney and brain too. A potential source of contamination of the aquatic environment is usage of plant protection formulations. No cases of pesticide acute poisoning have been reported in fish in the last decade, however, non-target organisms are exposed to pesticides, as many pesticide compounds are detected in surface water (Modrá & Svobodová, 2009)

The hazardous effects of pesticides on various metabolic pathways are a great problem for environmental health and should be well determined. As many biochemical pathways and processes are conserved across species, modes of pesticides action could predict analogous mechanisms of toxicity, target site(s), and (or) toxic effects for non-targeted species. A comparison of modes of action with biochemical and physiological effects in vertebrates and invertebrates indicates that f pesticides may be targeting the same or related biochemical and (or) physiological processes in non-targeted species (Elskus, 2012). Several researchers provide evidence supporting this view. Ochoa-Acuña et al., (2009)

suggest that the adverse effects of conazole fungicides in non-target species is mediated through cytochrome P450 pathways common across species. Strong evidence in support of such expectations is provided by Mazur & Kenneke, (2008) who report similar, and in some cases identical, in vitro metabolite profiles for conazoles in trout, rat, and human liver. The cytochrome P450 monooxygenase system metabolizes a large number of xenobiotic compounds including many environmental pollutants. This metabolism can lead to detoxification, or in some cases, activation to reactive intermediates with toxic and carcinogenic effects. Metabolism of xenobiotics occurs mainly through cytochrome P450 enzymes (CYPs). CYPs are a superfamily of hemoproteins, among which the CYP1, CYP2, and CYP3 families participate largely in the oxidative metabolism of xenobiotics (Verbueken et al., 2017). CYPs account for approximately 75% of the enzymes involved in the metabolism of marketed agrochemicals (Nawaji et al., 2020). About one quarter of the P450s are generally considered to be involved primarily in the metabolism of xenobiotic chemicals. The elimination of toxicant from the body is to a great extent determined by the action of cytochromes P450 (CYP) super family, of which predominant ones are CYP3A4, CYP2D6, CYP2C19, CYP2C9, and CYP1A2 (Wienkers & Heath, 2005).

A battery of CYP P450s is known to be regulated by various genes responsible for the biotransformation and xenobiotic metabolism in the organisms. Metabolism or biotransformation of xenobiotics occurs through phase I (cytochrome P-450 monooxygenase enzymes) and phase II (conjugating enzymes) pathway for detoxification and excretion of toxic chemicals. However, if either of the process are not completed the xenobiotic activates some intermediates that eventually results in toxicity, carcinogenicity, and other adverse effects (Zanette et al., 2009; Goldstone et al., 2009; Dorrington et al., 2012).

While such biochemical insights do not allow cross-species predictions of toxic potency, they do provide a first step towards identifying potential mechanism of action in aquatic invertebrates and fish for which mechanistic studies of many pesticides action have not been conducted. Pesticides such as Azoxystrobin have been reported to have an impact on respiration in fungi by inhibiting electron transport in mitochondria, leading to cellular oxidative stress. Recent studies indicate that azoxystrobin disrupts mitochondrial respiration in both fungi (Bartlett et al., 2002; Kim et al., 2008; Gisi & Sierotzki, 2008) and fish (Olsvik et al., 2010). Imidazoles, triazoles, and the pyrimidine fungicide fenarimol disrupts CYP450s in both mammals and fish (Ankley et al., 2005; Hinfray et al., 2006; Şişman & Türkez, 2010). Hence, in the present study an attempt is made to have an insight of oxidative stress by measuring CYP450 gene on exposure of AGs in ICG cells.

The effect of the environmental toxicants on the epigenome has attracted a considerable interest in the past few decades. Epigenetics refers to the modification of gene expression through changes in the chemical makeup of nucleotides or the associated histone proteins rather than alteration in the genetic code or DNA sequence itself. Three common alterations have been studied, including DNA methylation, histone modifications, and noncoding RNA expression. However, epigenetic modifications are not generally limited to these types of alterations. Incorporating the toxic-induced epigenetic alterations as informative factors in the risk assessment process is now rather fundamental given the role of epigenetic alterations in regulating gene and accordingly protein expression (Handy et al., 2011).

Epigenetic mechanisms are essential for development, cell differentiation, protection against viral genomes, and seem to be critical for the integration of

endogenous and environmental signals during the life of a cell or an organism. By analogy, deregulation of epigenetic mechanisms has been associated with a variety of human diseases, most notably cancer (Vaissière et al., 2008). Among epigenetic mechanisms, the covalent post-translational modifications of histone proteins are dependent on specific enzymes mechanism (Bannister & Kouzarides, 2011)

Exposure to a wide range of environmental chemicals has been shown to induce epigenetic changes in various models and is extensively reviewed by Feil & Fraga, (2012) and Jacobs et al., (2017). Despite the accumulating scientific evidence, epigenetic is not taken into consideration in any risk assessment framework so far because of limited result reproducibility as well as comprehensive understanding and standardization (Rasoulpour et al., 2011; Shaw et al., 2017). Nevertheless, epigenetic changes serve as predictive toxicity markers as they may represent very early molecular events that initiate the development of an adverse phenotype (Greally & Jacobs, 2013; Kim et al., 2012). Consequently, several position papers supported by the Organization for Economic Co-operation and Development (OECD) and the European Food Safety Agency (EFSA) stressed out the need to systematically investigate the epigenetic-related effects of chemicals (Rasoulpour et al., 2011; Greally & Jacobs, 2013; Marczylo et al., 2016; Blanc et al., 2019).

To achieve a significant reduction in animal testing as well as to increase the experimental throughput, alternative tests, including cell lines and unprotected animal early-life stages, are widely used in ecotoxicology. Bouwmeester et al., (2016) highlighted that specific DNA methylation changes can occur in advance to embryotoxic effects and, therefore, can be useful for toxicity-predicting screening. So far, only a limited number of studies have investigated the

epigenetic effects of chemicals in vitro in the context of environmental science. However, a few reports showed that cells and established cell lines in culture are also sensitive to DNA methylation changes induced by chemicals such as BPA, Benzo-a-Pyrene and the DNA-hypomethylating drug 5-azacytidine (Sadikovic & Rodenhiser, 2006; Bastos Sales et al., 2013; Farmen et al., 2014). In addition, the use of a cell line would allow to quickly and easily investigate the stability of epigenetic changes in a tissue-specific manner. Especially DNA methylation is mitotically inherited and its alteration in normal and pathological conditions has been extensively studied (Klutstein et al., 2016). Therefore, it appears as a good candidate to investigate the stability of toxic effects on regulatory mechanisms associated to potential adverse outcomes,

In recent times, the relationship between oxidative DNA damage and homeostasis of DNA methylation modification is found (Jiang et al., 2020). Induced oxidative stress by xenobiotics leads to DNA damage which further interrupts the binding of DNA methyltransferases (DNMTs) to CpG islands in DNA templates, resulting in abnormal methylation of cytosine in CpG dinucleotides (Jiang et al., 2020). DNA that contains 5-methylcytosine (5-mdC) can recognize proteins by enriching methylated nucleotides. 5-mdC blocks the binding of transcription factors to DNA templates, leading to chromatin compression and gene silencing (Vanaja et al., 2018; Thakur & Chen, 2019). DNA methylation is considered to be one of the most crucial epigenetic regulators of gene expression. However, epidemiological evidence shows that changes in DNA methylation are associated with exposure to multiple trace metals in the environment, including Pb, As and Ni (Martinez-Zamudio & Ha, 2011; Tchounwou et al., 2012). Furthermore, in vivo and in vitro assays have also demonstrated that exposure to metals, such as As, Pb, Cd and Hg, might have an

impact on global DNA methylation patterns (Sanchez et al., 2017; van der Ven et al., 2017; Wang & Yang, 2019). Thus, abnormal DNA methylation status can be a valuable tool to assess the adverse epigenetic effects of trace metals on organisms.

Hence, to further understand the functional interplay between mitochondrial dysfunction (cyp P450) and nuclear events, we examined epigenetic modification mediated methylation (dnmt) in ICG cell line on exposure of AGs.

### **3.2 Materials and Methodology**

#### **DAPI staining**

##### **Principle**

DAPI (4',6-diamidino-2-phenylindole) is a blue-fluorescent DNA stain that exhibits ~20-fold enhancement of fluorescence upon binding to AT regions of dsDNA. It is excited by the violet (405 nm) laser line and is commonly used as a nuclear counter stain in fluorescence microscopy.

**Method:** ICG Cells were seeded in 12-well plates (TPG12, HiMedia, India) and exposed to Low dose ( $IC_{50} / 20$ ), moderate dose ( $IC_{50} / 10$ ) and high dose ( $IC_{50} / 5$ ) of all AGs for 7 days. The cells were washed twice with PBS (M1866, pH 7.4, HiMedia, India), stained in DAPI dye (18668, SRL) liquor at a final concentration of 1 mg/ml, and incubated in dark for 15 min at 28 °C. After washing with PBS, samples were observed using a fluorescence microscope (Zeiss Axioplan-2 imaging fluorescence microscope).

##### **Total RNA Extraction (Trizol method)**

Total RNA was extracted isolated from ICG cells from control and treated cells for all agrochemicals. 500 µl TRIzol reagent (Invitrogen) was added in each well and scraped out in 1.5 ml RNase free tubes. For complete dissociation of nucleoprotein complexes, samples were incubated for 5 minutes at room

temperature. The incubation was followed by the addition of chloroform and was vigorously shaken for effective mixing of both the solutions. The samples were kept at room temperature for 5 minutes till the aqueous and organic layers were distinct. Thereafter, the tubes were subjected to centrifugation at 12,000x g for 15 minutes at 4°C. The mixture got separated into a lower red phenol-chloroform phase, an interphase, and a colourless upper aqueous phase. An aliquot of upper aqueous phase was then transferred into a new 1.5 ml micro centrifuge tube. Precipitation was done by adding 500 µl of isopropanol to the supernatant that was transferred. The samples were kept in room temperature for 10 minutes, centrifuged at 12,000x G for 15 minutes at 4°C. After precipitation the supernatant was discarded without disturbing the pellet and was washed in 500 µl of 75% ethanol and then 500 µl absolute ethanol was added to the pellet. Effective mixing was done by gentle inversion and was further subjected to centrifugation at 7,500 x g for 5 minutes at 4°C. The pellet was resuspended by adding 40 µl of DEPC water (Diethylpyrocarbonate), was quantified spectrophotometrically at 260nm using NanodropC and was stored in -20° C.

### **cDNA Synthesis**

First strand of cDNA was synthesized from each sample using Thermo Scientific Verso cDNA Synthesis Kit (AB-1453/A). Verso Reverse Transcriptase Verso is an RNA-dependent DNA polymerase with a significantly attenuated RNase H activity. Verso can synthesize long cDNA strands, up to 11 kb, at a temperature range of 42 °C to 57 °C. In reaction, 1 µg RNA was used as a template for cDNA synthesis using oligo dT primers. The volume of each component is for a 20 µl final reaction. The Reaction mix is mentioned in Table given below.

	Volume
5X cDNA synthesis buffer	4 $\mu$ l
dNTP Mix	2 $\mu$ l
anchored oligo dT /random hexamers	1 $\mu$ l
RT Enhancer	1 $\mu$ l
Verso Enzyme Mix	1 $\mu$ l
Template (RNA)	1-5 $\mu$ l
Molecular grade nuclease-free Water	To 20 $\mu$ l
Total Volume	20 $\mu$ l

Table 3.1 Reaction mix for cDNA synthesis

After setting up reaction mix, samples were kept in thermocycler in following conditions:

**Reverse transcription cycling program:**

	Temperature	Time	Number of cycles
cDNA synthesis	42 °C	30 min	1 cycle
Inactivation	95 °C	2 min	1 cycle

Table 3.2 Reverse transcription cycling program for cDNA synthesis

**RT-PCR Amplification**

Quantitative RT-PCR was performed using PowerUp SYBR Green Master Mix (A25741, Applied Biosystems, USA) in Quant Studio 12K (Life technology) FAST real-time PCR machine with primers to detect selected messenger RNA (mRNA) targets. The melting curve of each sample was measured to ensure the specificity of the products. GAPDH was used as an internal control to normalize

the variability in the expression levels and data was analyzed using  $2^{-\Delta\Delta CT}$  method (Livak and Schmittgen, 2001).

Component	Volume (20 $\mu$ L/well)
PowerUp SYBR Green Master Mix (2X)	10 $\mu$ l
Forward Primer (10uM)	1 $\mu$ l
Reverse Primer (10uM)	1 $\mu$ l
DNA Template	2 $\mu$ l
Molecular grade Nuclease free water	6 $\mu$ l
Total	20 $\mu$ l

Table 3.3 Real Time PCR Reaction mix

Step	Temperature	Duration	Cycles
UDG activation	50°C	2 minutes	Hold
Dual- Lock DNA polymerase	95°C	2 minutes	Hold
Denature	95°C	3 seconds	40
Anneal/extend	60 °C	30 seconds	

Table 3.4 Real Time PCR condition

	Gene Name	Primer Type	Sequence	Tm
1	gapdh	Forward	CTCACACCAAGTGTTCAGGACGAACAG	66.38
		Reverse	GTCAAGAAAGCAGCACGGGTCACC	66.13
2	P <sub>450</sub>	Forward	CCCAATTTCTGTGTCTGAGAGCCTTG	64.8
		Reverse	CAGCTTCTGGAGCCCTTCAGGAATC	66.26
10	Dnmt	Forward	TCAGCCTTCGTCAAAGACCC	59.35
		Reverse	TTCGCCTTCTTCTCTGCCTC	59.35

Table 3.5 PCR real time PCR primer sequences

**Sequencing:**

Sequencing is a method of DNA sequencing first commercialized by Applied Biosystems, based on the selective incorporation of chain-terminating dideoxynucleotides by DNA polymerase during in vitro DNA replication. Developed by Frederick Sanger and colleagues in 1977.

classical chain-termination method requires a:

1. single-stranded DNA template,
2. a DNA primer
3. a DNA polymerase
4. normaldeoxynucleosidetriphosphates (dNTPs)
5. modified di-deoxynucleotidetriphosphates (ddNTPs)

These dNTP's and ddNTP's lack a 3'-OH group required for the formation of a phosphodiester bond between two nucleotides, causing DNA polymerase to stop

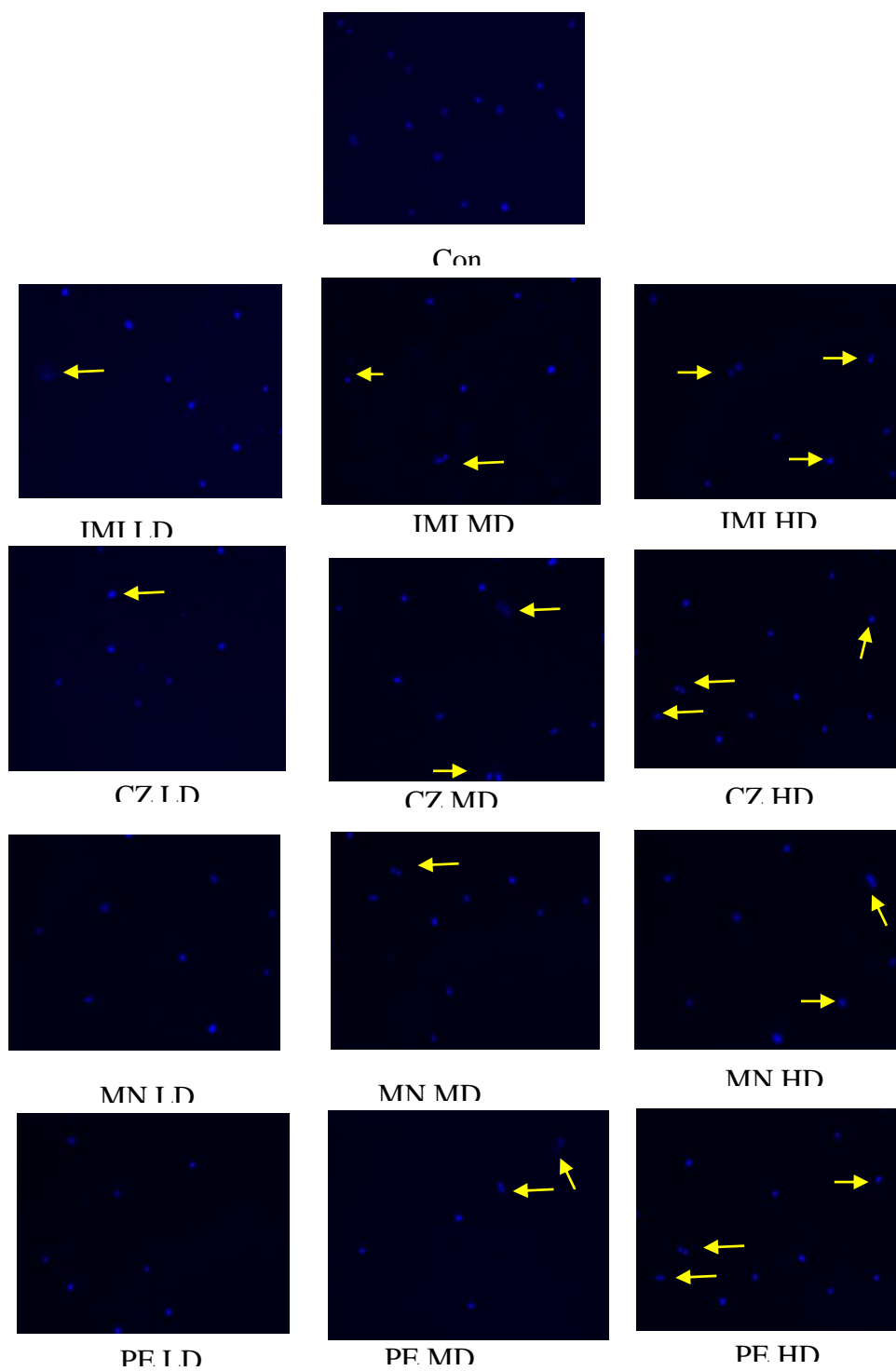
the extension of DNA when a modified ddNTP is incorporated. The ddNTPs may be radioactively or fluorescently labeled for detection in automated sequencing machines.

The DNA sample was divided into four separate sequencing reactions, containing all four of the standard deoxynucleotides (dATP, dGTP, dCTP and dTTP) and the DNA polymerase. To each reaction, added only one of the four dideoxynucleotides (dATP, ddGTP, ddCTP, or dTTP), while the other added nucleotides were ordinary ones. The dideoxynucleotide was added to be approximately 100-fold lower in concentration than the corresponding deoxynucleotide, allowing for enough fragments to be produced while still transcribing the complete sequence. Following rounds of template DNA extension from the bound primer, the resulting DNA fragments were heat-denatured and separated by size using gel electrophoresis. This was frequently performed using a denaturing polyacrylamide-urea gel with each of the four reactions run in one of four individual lanes (lanes A, T, G, C). The DNA bands were then visualized by UV light and the DNA sequence was directly read by gel image.

**Sequencing and Data analysis:** The amplified PCR product was purified by Purelink (Invitrogen), PCR purification column as per manufacture's instruction. The PCR amplicon was sequenced at thermo fisher scientific, 372 (Chromas,India). The PCR amplification and sequencing were also performed.

Using the clustalW, the nucleotide sequences of field isolates were matched with the sequences of known sequences. The BioEdit software v7.0.5.3 was used to analyze the aligned sequences. MEGA-X software was used to execute phylogenetic analysis of field isolates with known IBDV subtypes or vaccination strains using the neighbor-joining method with 1000 bootstrap repeats.





Nuclear Abnormalities	Exposure With IMI			
	Control	LD	MD	HD
Micronucleus	0.2± 0.02	0.2 ± 0.04	3.2 ± 0.09	6.3 ±0.01
Bi-nucleated cells	1.1±0.22	1.4± 0.72	2.2 ± 0.59	12. ±0.67
Lobed	0.2 ±0.53	10.8± 0.92	14.5± 0.92	18.7±0.24
<b>Total Abnormality</b>	1.4±0.1	12.4 ± 1.9*	19.9±6.4**	33.0 ± 0.9**

**Table 3.6: Frequency of Micronuclei and nuclear abnormalities counted in ICG cells when exposed to IMI for 7 days**

Nuclear Abnormalities	Exposure With CZ			
	Control	LD	MD	HD
Micronucleus	0.2 ± 0.02	0.2± 0.06	0.9 ± 0.09	4.8 ± 0.04
Binucleated cells	1.1 ±0.22	1.5±0.30	2.2±0.59	8.6± 0.59
Lobed cells	0.2 ±0.53	8.1±0.41	10.4±0.19	10.5± 0.92
<b>Total Abnormality</b>	1.4 ±2.1	9.6 ± 0.7	13.6 ± 0.9*	24.8 ±4.3**

**Table3.7 :Frequency of Micronuclei and nuclear abnormalities counted in ICG cells when exposed to CZ for 7 days**

Nuclear Abnormalities	Exposure With MN			
	Control	LD	MD	HD
Micronucleus	0.2 ± 0.02	0.1± 0.02	0.1± 0.02	0.1± 0.02
Binucleated cells	1.1 ±0.22	1.1±0.22	1.5±0.30	1.3±0.22
Lobed cells	0.2 ±0.53	0.24±0.43	0.4±0.41	1.9±0.53
<b>Total Abnormality</b>	1.4 ±2.1	1.4 ±0.1	2.1 ±0.7	3.3 ±1.1

**Table 3.8 Frequency of Micronuclei and nuclear abnormalities counted in ICG cells when exposed to MN for 7 days**

Nuclear Abnormalities	Exposure With PE			
	Control	LD	MD	HD
Micronucleus	0.2 ± 0.02	0.1± 0.02	0.2± 0.06	0.5± 0.09
Binucleated cells	1.1 ±0.22	1.3±0.22	1.5±0.30	3.2±0.59
Lobed cells	0.2 ±0.53	4.9±0.53	5.1±0.41	7.0 ±0.19
<b>Total Abnormality</b>	1.4 ±2.1	5.2±1.1	6.8 ±1.7	10.7±1.1*

**Table 3.9 Frequency of Micronuclei and nuclear abnormalities counted in ICG cells when exposed to PE for 7 days**

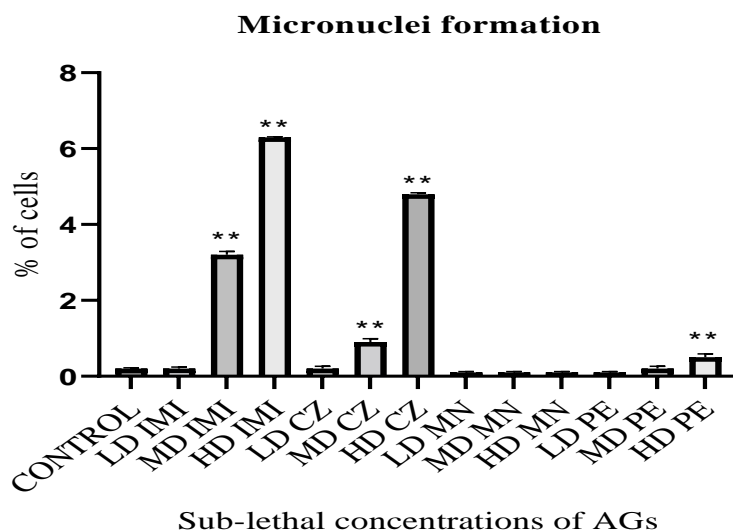


**Figure 3.3** represents frequency micronuclei formation in ICG cells exposed to AGs. Each value represents the mean  $\pm$  SEM. (n=3), Significant level indicated by \* $p < 0.05$ ; \*\* $p < 0.01$

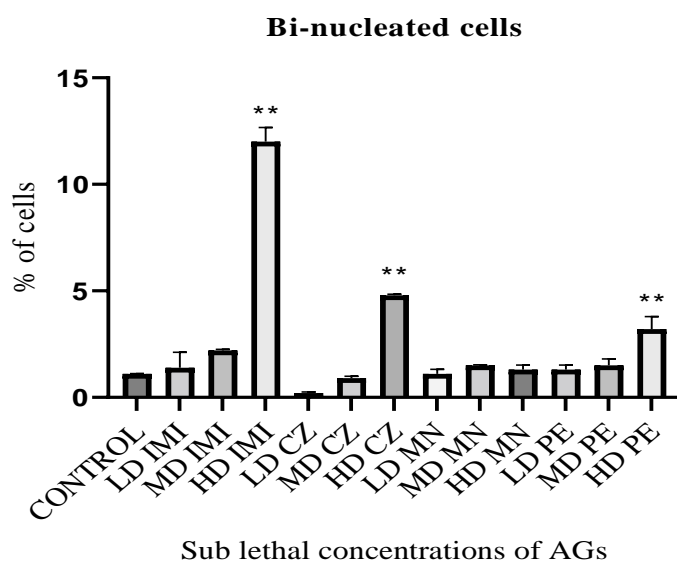


**Figure 3.4** represents frequency micronuclei formation in ICG cells exposed to AGs. Each value represents the mean  $\pm$  SEM. (n=3), Significant level indicated by \* $p < 0.05$ , \*\* $p < 0.01$

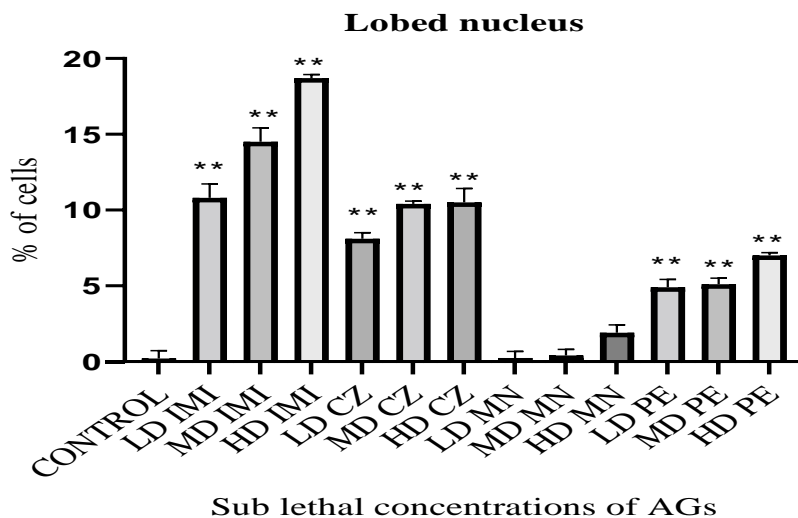


Figure 3.5 represents frequency micronuclei formation in ICG cells exposed to AGs. Each value represents the mean  $\pm$  SEM. (n=3), Significant level indicated by \* $p < 0.05$ ; \*\* $p < 0.01$

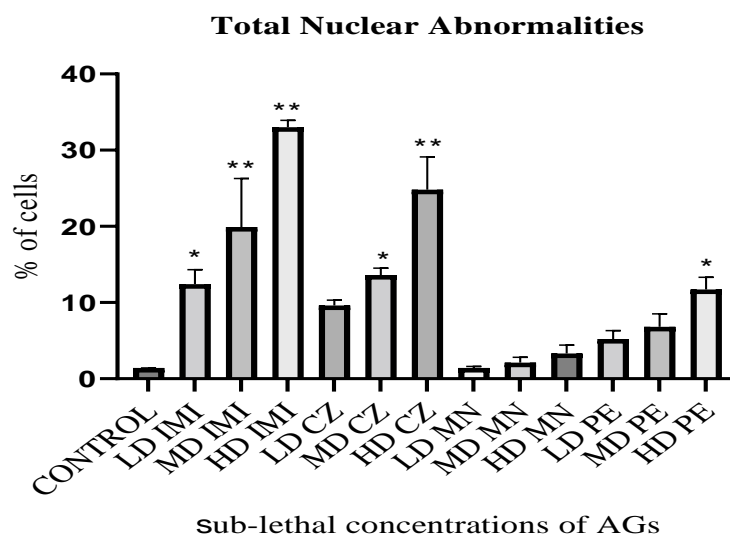


Figure 3.6 represents the total nuclear abnormalities in ICG cells exposed to AGs. Each value represents the mean  $\pm$  SEM. (n=3), Significant level indicated by \* $p < 0.05$ ; \*\* $p < 0.01$

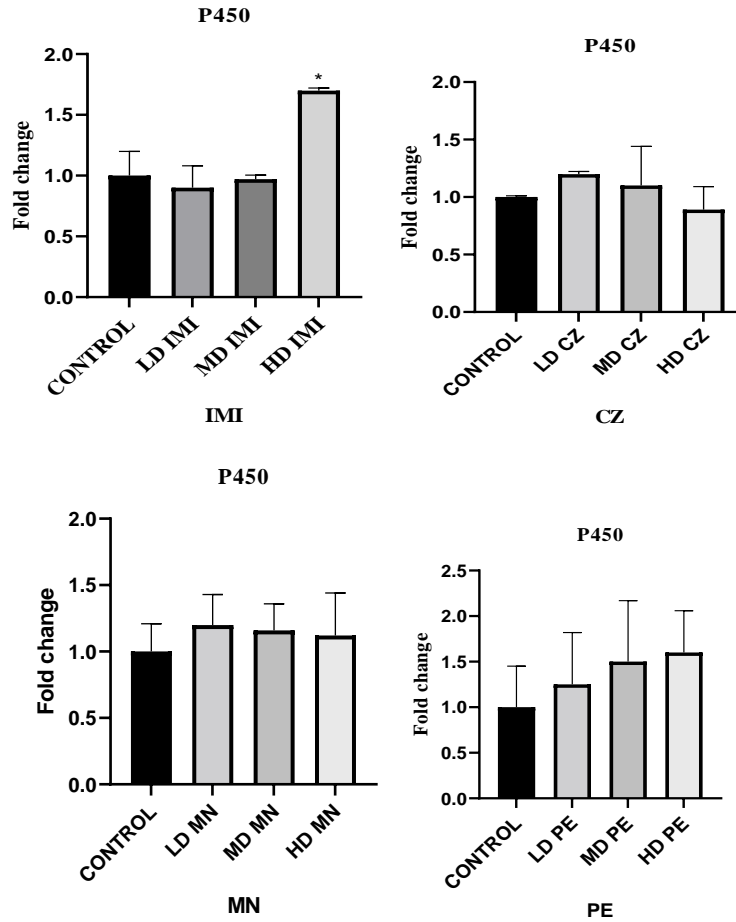
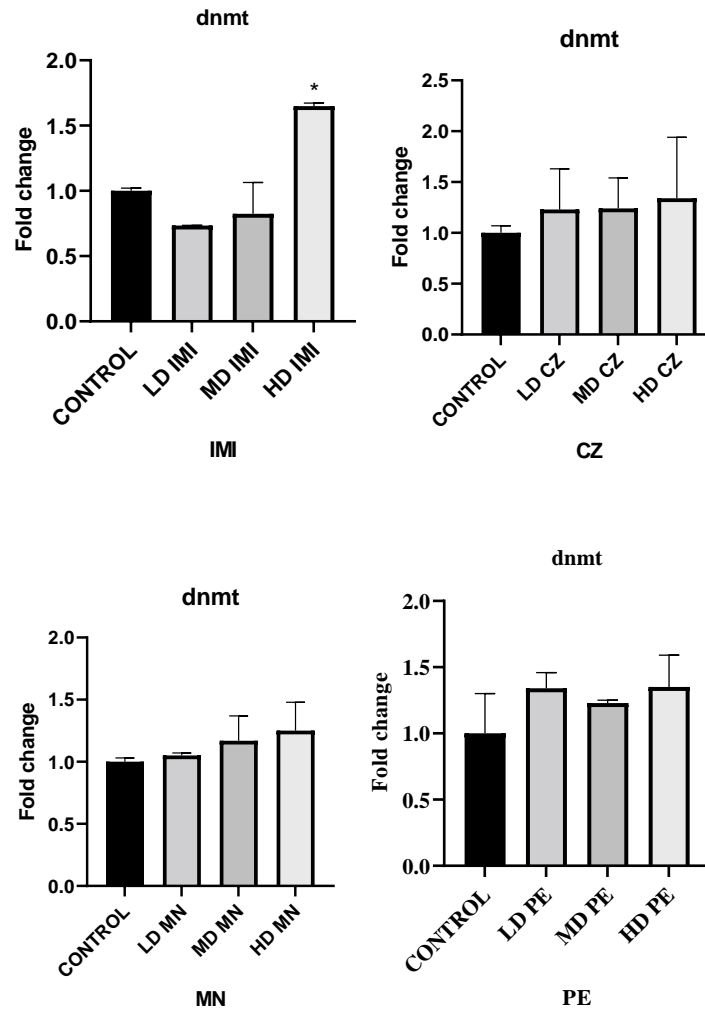


Figure 3.7: Depicts the level of P450 (in folds) in ICG cells treated with sub-lethal doses of IMI, CZ, MN and PE. Each value represents the mean  $\pm$  SEM. (n=3), Significant level indicated by \* $p < 0.05$



3.8 Depicts the level of dnmt (in folds) in ICG cells treated with sub-lethal doses of IMI, CZ, MN and PE. Each value represents the mean  $\pm$  SEM. (n=3), Significant level indicated by \* $p < 0.05$

Agrochemicals	P450	dnmt
Control	1±0.2	1.0±0.02
LD IMI	0.9±0.18	0.73±0.002
MD IMI	0.97±0.03	0.83±0.240
HD IMI	1.7±0.002*	1.65±0.02*
LD CZ	1.2±0.003	1.23±0.40
MD CZ	1.1±0.3	1.24±0.30
HD CZ	0.89±0.20	1.34±0.60
LD MN	1.2±0.2	1.05±0.020
MD MN	1.16±0.2	1.17±0.20
HD MN	1.12±0.32	1.25±0.23
LD PE	1.2±0.57	1.34±0.12
MD PE	1.50±0.67	1.23±0.02
HD PE	1.6±0.5	1.35±0.24

**Table 3.10 depicts the mean± SEM values of Folds change in p450 and dnmt gene in ICG cell line exposed o AGs**

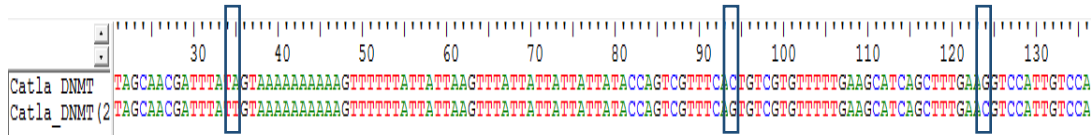


**Figure 3.9: Nucleotide sequence alignment of the dnmt region between nucleotide 21-134 of known sequence for dnmt for *C. catla* and cells treated with IMI for 7 days**

Multiple sequence alignment of the dnmt region from treated cells suggested its similarity with the known very virulent strains reported earlier. However, there are transverse A35T, C94G and G124C.

**Maximum Likelihood Estimate of Transition/Transversion Bias**

The estimated Transition/Transversion bias (R) is 0.00. Substitution pattern and rates were estimated under the Kimura (1980) 2-parameter model (Kimura et al 1980). The nucleotide frequencies are A = 25.00%, T/U = 25.00%, C = 25.00%, and G = 25.00%. For estimating ML values, a tree topology was automatically computed. The maximum Log likelihood for this computation was -975.700. This involved 3 nucleotide sequences. Codon positions included were 1st+2nd+3rd+Noncoding. There were a total of 680 positions in the final dataset. Evolutionary analyses were conducted in MEGA X (Kumar S., et al 2018).

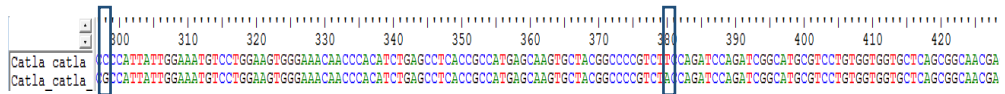
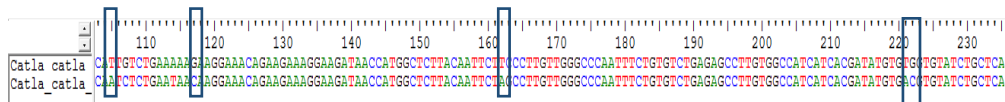


**Figure3.10: Nucleotide sequence alignment of the P450 region between nucleotide 104-235 and B) 297-424 of known sequence for P450 for *C. catla* and cells treated with IMI for 7 days**

Multiple sequence alignment of the P450 region from treated cells suggested its similarity with the known very virulent strains reported earlier. However, there are transverse T105A, G117C, T162A, G222C, C298G and T380A.

#### Maximum Likelihood Estimate of Transition/Transversion Bias

The estimated Transition/Transversion bias (R) is 0.00. Substitution pattern and rates were estimated under the Kimura (1980) 2-parameter model (Kimura et al 1980) The nucleotide frequencies are A = 25.00%, T/U = 25.00%, C = 25.00%, and G = 25.00%. For estimating ML values, a tree topology was automatically computed. The maximum Log likelihood for this computation was -3640.927. This analysis involved 3 nucleotide sequences. Codon positions included were 1st+2nd+3rd+Noncoding. There were a total of 2566 positions in the final dataset. Evolutionary analyses were conducted in MEGA X (Kumar S., et al 2018).

#### **3.4 Discussion:**

Different toxic endpoints and different fish cell lines have been employed to evaluate the toxicity of the pesticides. Previous studies from our lab has reported the ability of these AGs to damage liver, Kidney, Muscle and gills and have induced enzymatic responses in *O.mossambicus* and *L.rohita*, associated with the disruption of normal fish behaviour and physiology in in vivo conditions. A major occurrence in cells exposed to toxic chemicals is DNA damage. Nucleotide sequence can be altered when DNA lesions occurs at specific sites of the gene, setting off the process of mutation and some other cellular responses (Lord & Ashworth, 2012). Micronucleus assay is used to detect chromosomal damage in once-divided bi-nucleated cells, which contain micronuclei and other cellular abnormalities. The frequency in the occurrence of micronuclei is a reflection of cytotoxicity indicating breakage in chromosome and/or total chromosome loss (Ayanda et al., 2021; Xin et al., 2014). In the present

study, sub-acute concentrations of AGs (IMI, CZ, PE and MN) were able to induce micronuclei formation (MN) and various other cell abnormalities like apoptosis, bean-shaped cell and lobed, notched nuclei in ICG cells. This corroborates the findings of previous researchers (Upadhyay A et al., 2016) who have reported cytogenetic effects of herbicide in fish. This study also reveals that the higher the dose of the herbicide PE administered, the higher the frequency of nuclear abnormalities. An increase in the number of micronuclei in peripheral blood of *O. mossambicus*, with increasing dose was reported by the same group on exposure to PEI. An increase in micronuclei frequency in *Channa punctata* (Bloch) was also reported with increasing concentrations of chlorpyrifos after acute exposure (Kumar et al., 2012), Genotoxicity assessment of acute exposure of chlorpyrifos to freshwater fish *Channa punctatus* (Bloch) using micronucleus assay and alkaline single-cell gel electrophoresis. *Chemosphere* 2008; 71: 1823–1831. Nuclear abnormalities in the present study (bean-shaped cell and lobed & notched nuclei) reported was previously reported by other authors (Monteiro et al., 2011; I. O. Ayanda et al., 2018).

It has been found that changes in the morphology of the nucleus is a product of exposure to xenobiotic contaminants, originating from a genotoxic event.<sup>53</sup> Low induction of micronuclei in fish blood have previously been reported (Winter et al., 2007). Formation of micronuclei in erythrocytes of the fathead minnow (*Pimephales promelas*) after acute treatment with mitomycin C or cyclophosphamide. on exposure of fish to environmental contaminants. Carbazole induced toxicity to embryos of *Danio rerio* has also been proved to show the highest potency for micronuclei formation in RTL-W1 cells (Brinkmann et al., 2014; Hinger et al., 2011). Some heterocyclic aromatic compounds are Ah receptor agonists in the DR-Calux and the EROD assay with RTL-W1 cells.

Jiraungkoorskul et al., (2007) have opined that micronuclei are aberrant nuclei produced during impaired mitosis and their occurrence is a simple diagnostic tool to determine the clastogenicity/mutagenicity of substances. Thus our studies are in line of previous reports of using Micronuclei test as one of the important investigative method to prove the genotoxicity of AGs.

The next target was focused on induction of the xenobiotic metabolizing enzyme cytochrome P450 1A (Cyp1a) as a biomarker of exposure and an adaptive cellular response. Cyp1a induction is a downstream event following aryl hydrocarbon receptor activation, which occurs through binding of a number of endogenous and exogenous ligands (Denison & Nagy, 2003). It has been reported that even at low levels, benzo(a)pyrene is a potent inducer of Cyp1a activity, with naïve killifish demonstrating significantly increased Cyp1a enzymatic activity after exposure to concentrations as low as 10 µg/L (39.6 nM) (Lee & Anderson, 2005; Verma et al., 2012; Wills et al., 2009). Increased basal metabolic capability has been detected in fish adapted to highly contaminated sites and is associated with differences in DNA damage (Wills et al., 2010). Both enzymatic activity and gene expression levels have been used as biomarkers in field and experimental studies to provide a quantitative measure of exposure to xenobiotics (Costa et al., 2013; Kopecka-Pilarczyk & Schirmer, 2016; Gubbins et al., 2000).

Based on accumulating experimental data role of AhR can be broadly categorized in three important pathways. The first is the extrinsic AhR xenobiotic signaling pathway, which usually requires an exogenous ligand for activation and results in the induction of several Phase I and Phase II metabolizing genes. A second network of pathways involves the interaction of the AhR with various cell-signaling proteins, such as Rb and E2F in the presence or absence of an inducer. The third pathway is the intrinsic AhR pathway, which remains elusive, in terms

of exact mechanism of action and is thought to be dependent on an endogenous ligand and play key roles in important physiological and developmental processes. The pathways are likely to interact with one another, proving that the exact function of the receptor is a lot more complex, than initially thought (Androutsopoulos et al., 2009). The PLHC-1 cell line, originally derived from an hepatocellular carcinoma induced in the teleost fish *Poeciliopsis lucida*, is known to have functional AhR-dependent pathways that are activated by polycyclic aromatic hydrocarbons and dioxin-like compounds resulting in induced Cyp1a expression and activity (Thibaut et al., 2009; della Torre et al., 2011; Gulden & Seibert, 2006; Kienzler et al., 2012).

In the present study a significant dose dependent increase in the expression of P450 was observed on exposure of AGs on the ICG cell line. Increased levels of Cyp1a and associated with decreased cell number were observed to be maximum for all the AGs, however, it was maximum in IMI and CZ compared to PE and MN. Meyer et al., (2002) have reported an altered expression and relationship of P450 has been reported for survival in contaminated sediments in killifish (*Fundulus heteroclitus*). AhR mediated CYP1A1 induction leads to activation of certain Phase II xenobiotic metabolizing enzymes, which has been well established, however, recent discoveries have illuminated a wider function of AhR, than initially thought. It is now generally accepted that the receptor is involved in physiological functions beyond xenobiotic metabolism, such as regulation of cell growth, apoptosis, hypoxia signaling, cell adhesion and matrix metabolism (Puga et al., 2009; Kung et al., 2009).

The aryl hydrocarbon receptor (AhR) pathway as a regulatory pathway for cell adhesion and matrix metabolism. Kung et al., (2009) in their studies has confirmed the Potentiating effect of graphene nanomaterials on aromatic

environmental pollutant-induced cytochrome P450 1A expression in the topminnow fish hepatoma cell line PLHC-1. Furthermore, slight induction of the *cyp1a* gene has been also reported in a rainbow trout gonad cell line (RTG-2) (Torre et al., 2011).

Processes of apoptotic signalling are associated with variations of apoptotic molecules, including cytochrome c and p53 (Zhao et al., 2009). When the cell has been in an apoptotic state, p53 activation is an effective indicator and/ as well as the release of the cytochrome c into the cytosol from the mitochondria. Besides, the reduction in the Bcl-2 is considered a significant correlation in cell death or apoptosis. Apoptotic protease activating factor-1 (Apaf1) interacts with cytochrome c in the cytosol to activate caspase 9. Then, this initiator caspase activates one of the important regulators of apoptosis, Cas3 (chapter II).

Thus, based on literature data and our results there is no doubt that CYP induces toxicity impact which is demonstrated by induced apoptosis through up-regulation of p450 and Cas3 besides the down-regulation of Bcl2 expression in the ICG cell line. These effects are because of CYP induced oxidative stress which can cause lipid peroxidation, cell structure damage and eventually induce DNA damage and apoptosis (Indrayanti et al., 2019). Effects of per oral cypermethrin exposure on Bcl-2 expression in granulose cells and antral follicle count of *Rattus norvegicus* ovaries (Indrayanti et al., 2019). These have also been demonstrated by Abd El-Hameed & Mahmoud, (2020).

Our results suggest that IMI and CZ has influenced the cells homeostasis first of all via oxidative stress, reducing the cell response and defense capacity and affecting its energetic levels. This situation of stress and energy imbalance could represent a condition that, modifying some of the analyzed biochemical pathways, would predispose to cellular transformation (Ruiz et al., 2019), and that

---

ICG cell lines overexpressing CYP1 may be a valuable model to characterize the biochemical and toxicological properties of CYP1.

Phenotypic plasticity, by which prolonged or repeated stress exposure leads to changes in phenotypic responses that optimize physiological performance, has been observed in fishes and this allows them to survive in rapidly changing environments (Crozier & Hutchings, 2014; Seebacher et al., 2015; Beaman et al., 2016). Many fish species have evolved molecular mechanisms and strategies that operate at the transcript level, and enable them to respond and adapt to these environmental stressors (Larsen et al., 2012). Although it is still not well-understood how signals of environmental stressors are perceived and integrated into the genome, there is growing evidence that epigenetic mechanisms (e.g., DNA methylation) play an essential role in facilitating this phenotypic plasticity through the modulation of gene expression (Eirin-Lopez & Putnam, 2021; McCaw et al., 2020; Ryu et al., 2020; Venney et al., 2020).

Epigenetic modifications are a dynamic combination of DNA methylation, histone modifications, and non-coding RNAs that regulate gene expression (Best et al., 2018; Eirin-Lopez & Putnam, 2021). DNA methylation is the reversible addition of a methyl group (CH<sub>3</sub>) to the 5' carbon end of cytosine (5mC) nucleotides catalyzed by specific DNA methyltransferases (Edwards et al., 2017). Thus, the temporal relationship between environmentally induced DNA methylation changes and gene expression appears to be complex (Beemelmans et al., 2021). Recent research provides compelling evidence that teleost DNA methylation is influenced in various ways by toxicants (Campos et al., 2013; Ventura et al., 2017; Beemelmans et al., 2021; Burgerhout et al., 2017; Metzger and Schulte, 2017; Ryu et al., 2018; Uren Webster et al., 2018; McCaw et al., 2020; Valdivieso et al., 2020). Nonetheless, the role of DNA methylation in

regulating gene expression following AGs exposure (IMI,CZ,MN,PE) is still largely unexplored.

A Mutation occurs when a DNA gene is damaged or changed in such a way as to alter the genetic message carried by that gene. mutations are essential raw materials for evolution(Loewe & Hill, 2010). As defined by Hershberg, (2015), DNA mutations is a single nucleotide changes in the DNA sequence of an individual organism which does not get refurbished by the cellular repair systems. Once a mutation occurs and is present within an individual, it will either increase in frequency within the population, or will vanish from the population. On the other side, DNA substitutions are those mutations that can be directly observed when we consider DNA sequence data. The substitutions observed may reflect the mutations that have occurred for better or worse, depending on how natural selection has affected them. For example, if when comparing sequences we observe that a certain substitution type (e.g., C to T transitions) occurs more frequently, this could either mean that this mutation type occurs more frequently, or that natural selection tends to favor this mutation type and it can be called as base-change mutation (Graur and Li 2000).

In the present study cytochrome P450 (P450, CYP) gene did show a significant upregulation in the ICG cells exposed to IMI, hence it was thought worthwhile to look into whether any alterations in the nucleotide sequence has occurred. Many toxicants have been proved to influence the expression of the cytochrome P450 (Guengerich and Rendic 2010; Rendic and Guengerich 2012; Guengerich 2017). Among different tissues of *C. catla*, the CYP1A expression has also been observed in kidney, liver, gill, muscle, intestine and brain (Kavita Kumari 2016). The occurrence of mis-sense mutation in humans has been analysed for the interpretation of mutations in P450 to understand their role in the

disease development and individual susceptibility to environmental cues (Fechter & Porollo, 2014).

In the present study sanger sequencing data showed occurrence of point mutation at six places (T105A, G117C, T162A, G222C, C298G and T380A), where T to A nucleotide base were more frequent followed by G to C and replacement of C to G was observed only once. As per the earlier reports more the frequency in the replacement of the base on IMI exposure has resulted into base change mutation. However, this needs to be validated further by *in vivo* studies and in the natural systems to conclude the exact epigenetic modifications occurred due to the toxic effect of xenobiotics.

Aquatic organisms such as fish are, in most cases, exposed to multiple stressors that are either natural or anthropogenically introduced into their environment (Dorts et al., 2016). Environmental factors or toxicants can promote phenotypic variation through alterations in the epigenome and facilitate adaptation of an organism to the environment (Kelley et al., 2021). DNMT1, DNMT3A and DNMT3B are three recognized types of DNA methyl transferases which are known to execute the genomic methylation process (Hamidi et al., 2015).

DNA methylation is one of the most important epigenetic modifications (Ley 2010) playing key roles in the regulation of gene expression, genomic imprinting, X chromosome inactivation, and tumorigenesis (Smith et al., 2013). DNA methylation is sensitive to the effects of environmental stressors and has been reported to increase the expression of stress genes as well as *dnmt3* suggesting its impact on the establishment of DNA methylation patterns (Dorts et al., 2016). Alterations in *dnmt* gene in ICG cells exposed to HD of IMI thus suggest genotoxic effect of IMI which is in agreement with the earlier reported

work (Dorts et al., 2016), as well as of Zhang et al., (2014) where they have concluded and correlated the association of DNA methylation with changes in gene expression, signal transduction and stress response after exposure to a wide range of exogenous compounds.

Hence, the result of the present study is suggestive of the similar mechanism by which IMI is probably influencing in its genotoxic expression. However, to illustrate and confirm the mechanism the generation studies will throw more light to interpret role of IMI in epigenetics.

### **3.5 Conclusion:**

Overall, putting all the results it can be concluded that:

1. The exposure of AGs has led to formation of nuclear abnormalities in which micronucleus formation, bi-nucleated and lobed nucleated cells were highest at HD of IMI followed by CZ and PE suggesting its genotoxic potential of AGs in ICG cells.
2. The significant alteration in expression and sequences of p450 and dnmt was reported in ICG cells exposed to HD of IMI suggest the probability of its role in toxicity leading to epigenetic alterations.